Richard Volpe
The Jet Propulsion Laboratory
California Institute of Technology
Pasadena, California 91109

Pradeep Khosla
Department of Electrical and Computer Engineering
The Robotics Institute
Carnegie Mellon University
Pittsburgh, Pennsylvania 15213

A Theoretical and Experimental Investigation of Impact Control for Manipulators

Abstract

This article describes a simple control strategy for stable hard-on-hard contact of a manipulator with the environment. The strategy is motivated by recognition of the equivalence of proportional gain explicit force control and impedance control. It is shown that negative proportional force gains, or impedance mass ratios less than unity, can equivalently provide excellent impact response without bouncing. This result is indicated by an analysis performed with an experimentally determined arm/sensor/environment model. The results are corroborated by experimental data from implementation of the control algorithms on the CMU DD Arm II system. The results confirm that manipulator impact against a stiff environment without bouncing can be readily handled by this novel control strategy.

1. Introduction

There are two extreme modes of operation for a manipulator: position-controlled motion through free space, and force-controlled interaction while constrained by the environment. Obviously the manipulator must change from one mode to the other readily. Usually, switching from constrained force control to unconstrained position control presents no problems. However, switching from free space motion to constrained force control has the significant problem of impact forces (Paul 1987). These forces can be very large and can drive an otherwise stable controller into instability. Typically, it is the force control strategy that must deal with this transient phenomenon, as the large force does not occur until after contact has occurred. However, the natural elasticity of the impact, or the response of the force controller to the transient, can cause the manipulator to rebound from the environment. Thus, the manipulator is once again unconstrained. This phenomenon can establish oscillatory behavior or, worse, drive the manipulator unstable. Obviously it is the goal of any controller to pass through this transitory period successfully and have the manipulator stably exerting forces on the environment. The controller must therefore pass through the impact phase by attempting to maintain contact with the environment until all of the energy of impact has been absorbed. A novel method of *impact control* to maintain stability and contact during this phase is presented in this article.

Previous research in force control has treated the impact phase as a transient that is dealt with by the same controller used to follow commanded force. The form of the force controller is typically an explicit force or impedance controller (Whitney 1985; Volpe 1990). In this article it will be shown that the best implementation of these strategies for force following is insufficient for impact control. However, the impact controller presented here still fits into the same framework. To understand this, the previous schemes will be briefly discussed and their weaknesses revealed. Then a newly proposed impact control strategy will be presented in the context of explicit force control and impedance control. An analysis will explain how the strategy provides stability, and experimental results will demonstrate its effectiveness.

2. Previously Proposed Methods For Impact Control

Most previous work in impact control has not employed any changes in the force controller structure (variation of gains or controller type). Instead, the impact phase is treated as a transient that must be dealt with by the force controller and the chosen gains, once contact has been established. Typically, modification of the control strategy

This work was completed while Volpe was a member of the Department of Physics, The Robotics Institute, Carnegie Mellon University, Pittsburgh, Pennsylvania, 15213.
The International Journal of Robotics Research,
Vol. 12, No. 4, August 1993, pp. 351–365,
© 1993 Massachusetts Institute of Technology.

has been attempted through active damping and/or passive compliance and damping.

2.1. *Maximal Active Damping*

One proposed method of dealing with the impact problem is to employ maximal damping during the impact phase (Khatib and Burdick 1986). Any force controller may be used; proportional control was used in this reference. The goal of this strategy is to damp out the oscillations caused by the transition. This may be successful for soft environments, but stiff environments have oscillations with small amplitudes and high frequencies. This makes damping difficult for three reasons. First, changes in position of the environmental surface may be smaller than the resolution the manipulator's position measurement devices. In this case, no velocity will be sensed. Second, for fast oscillations the calculated velocity signal will lag behind its ideal value, and the damping force may cause instability by being applied out of phase with the true velocity of the surface (Volpe 1990). Third, flexion in the links as a result of impact can slightly change the arm structure, thereby making the kinematics and velocity signal computation erroneous. These problems are compounded by the fact that the stiff environment that causes them will also cause a larger impact force and need stabilizing compensation all the more. Thus, this scheme may fail when most needed.

2.2. *Passive Compliance and Damping*

Another method for absorbing the shock of impact is to use passive compliance either on the end effector or in the environment. Some researchers have proposed the use of soft force sensors (Roberts 1984; Xu and Paul 1988). Another suggests the use of compliant "skin" for the force sensor (An and Hollerbach 1987). These methods appear to provide stable impact in two ways. First, the material used naturally provides passive damping that helps absorb some of the energy of impact, without the resolution or time lag problems of active damping. Second, the compliance of the material effectively lessens the stiffness of the system composed of the material and the environment. Following from the argument of the previous paragraph, this lessening of the stiffness helps active damping work. Because the end effector remains in contact with the environment over a larger range of displacement for the same experienced force, the displacement will not be below the resolution of the arm's position (and therefore velocity) measurement devices. Also, the frequency of oscillation will be less, reducing the phase lag of the computed velocity that is needed for active damping.

However, there are problems with passive compliance. First, it may not be modified without physical replacement of the material. Second, it limits the effective stiffness of the manipulator during position control. Third, it eliminates precise knowledge of the position of the environment. Fourth, it limits the forces that may be applied: beyond a certain range of operation, the compliant material is not linear and is prone to physical failure.

2.3. *Integral Explicit Force Control*

Integral force control acts as a low-pass filter (Youcef-Toumi and Gutz 1989; Volpe 1990; Vischer and Khatib 1990). Thus, for impact transients, the high-frequency components are filtered effectively. For impacts with low energy or with an inelastic environment, this may be sufficient. Otherwise, bouncing may occur. Results consistent with this interpretation have been reported (Youcef-Toumi and Gutz 1989). However, they contradict our results obtained with the CMU DD Arm II and reported later in this article. We show that integral control is very oscillatory (at best) during impacts. This is because of the nonlinear loss of contact with the surface and subsequent integrator wind-up, both of which cause severe hopping on the surface.

2.4. *Impedance Control and Proportional Explicit Force Control*

It has been analytically and experimentally demonstrated that impedance control against a stiff environment is equivalent to proportional gain explicit force control with feedforward (Volpe 1990; Volpe and Khosla 1991a,b). These schemes have been tried by many researchers (Khatib and Burdick 1986; Youcef-Toumi 1987; Kazerooni 1987; Hogan 1987; An and Hollerbach 1987). However, the gain in these implementations is not tuned for the best impact response. For explicit force controllers, the gain is tuned for optimal command following once contact has been established. Equivalently, the mass ratio of impedance control is chosen to obtain the desired inertia for free space motion or force exertion, but not impact. The result is an oscillatory system in which bouncing occurs after impact. This is consistent with simulation and experimental results (Eppinger and Seering 1987; An and Hollerbach 1987; Volpe 1990). A solution to this problem is to use a different proportional gain for the impact phase. To understand the proper choice for the gain values, it is necessary to analyze both explicit force control and impedance control schemes with a proper system model. This model is reviewed next, followed by a review of the force control strategies.

3. Arm/Sensor/Environment Model

The physical system employed in this study is depicted in Figure 1. The environment is a cardboard box with an aluminum plate resting on it. The measured stiffness of this environment is $\sim 10^4$ N/m. The box is resting on a table that is considerably more stiff than the box and is therefore considered ground for these tests. The force sensor is mounted on link 6 of the CMU DD Arm II; it has a measured stiffness of 5×10^6 N/m. Attached to the force sensor is a steel probe with a brass weight on its end. The brass weight serves as an end-effector substitute and provides a flat, stiff surface for applying forces on the environment. Previous analysis has indicated that a fourth-order model of this arm/sensor/environment is necessary and sufficient for force control. This section presents a review of the development of this model. Full details may be found in Eppinger and Seering (1986), Volpe (1990), and Volpe and Khosla (1990).

The dynamics of an n-DOF, serial link manipulator are described by a set of nonlinear, coupled differential equations (Fu et al. 1987). Included in this description are Coriolis and centripetal forces, as well as viscous damping and gravitational loading. However, these elements of the description may not always be significant. For instance, Coriolis and centripetal forces are not present when the manipulator is statically exerting force on the environment; viscous damping is not present in direct drive motors; and gravitational loading is not present for a space-based robot. Further, active compensation can remove the torques caused by these physical effects. For instance, calculation of the inverse dynamics of the arm removes the effects of gravity loading and Coriolis and centripetal forces (Khosla 1986), and negative damping gains can remove the effects of viscous friction (Colgate and Hogan 1988).

Therefore, for the purpose of this article the most important component of the dynamic description of the manipulator is its inertia. All other nonlinear components of the description will be ignored and assumed to be insignificant or compensated for. Further, by the appropriate transformation the description of the manipulator dynamics may be represented in Cartesian space (Khatib and Burdick 1986). If the task frame in Cartesian space is aligned with the principal axes of the inertia tensor, the dynamic description becomes fully decoupled. In this case, a single degree of freedom may be considered independently.

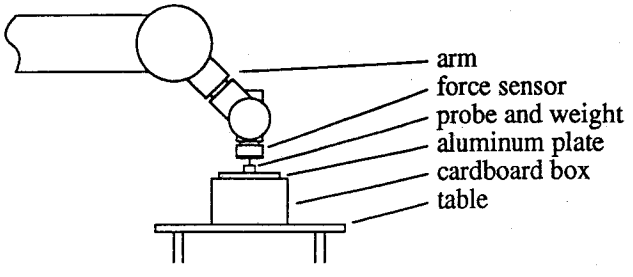

Fig. 1. The setup for the experiments.

The most basic one-DOF model of a manipulator is a second-order model that has a single mass, damping, and stiffness for the manipulator. The mass is configuration dependent and represents the effective manipulator inertia in that degree of freedom. The damping, if it exists, is a combination of the projection of the viscous joint damping into Cartesian space and the active damping, which may be performed directly in Cartesian space. The stiffness is due to the combination of mechanical and actively applied stiffnesses. The mechanical stiffness can come from either the links or the actuators. For now, we will ignore the link stiffness and consider the links to be pure transmitters of force. Actuator stiffness typically comes from gearing which is non-backdriveable. Many manipulators are backdriveable and do not exhibit mechanical stiffness. The CMU DD Arm II has no joint friction or gearing, and therefore, damping and stiffness will only be present if provided actively (Khosla 1986).

Having introduced a model of the manipulator, it is necessary to discuss an environmental model. Some researchers have made no assumptions about the structure of the environment, and have assumed instead that interaction with it will produce measurable forces (Salisbury 1980; Hogan and Cotter 1982; Hogan 1985; Maples and Becker 1986; Kazerooni et al. 1986; Goldenberg 1988). Other researchers, usually those working with a compliant system or sensor, have modeled the environment as a mechanical ground (Xu and Paul 1988; Sharon et al. 1989). Still others have recognized that the environment has some compliance and therefore have modeled it as a simple stiffness (Whitney 1977, 1985; Paul and Wu 1980; Raibert and Craig 1981; Khatib and Burdick 1986; De Schutter 1987, 1988; Youcef-Toumi 1987; Kahng and Amirouche 1988; Lawrence 1988; Ishikawa et al. 1989). Finally, some researchers have modeled the environment as a complete second-order system with components of mass and damping, as well as stiffness (Kazerooni et al. 1986; Eppinger and Seering 1987; Youcef-Toumi and Gutz 1989). This last form of the environmental model recognizes that the environment has oscillatory modes of its own but simplifies the overall analysis by only considering the first mode. Thus, the second-order model is more restrictive than just a general environment that exerts measurable force on the arm. However, the specific representation of the model's dynamic components will permit a better understanding of the interaction between the arm and the environment.

Between the arm and the environment exists the force sensor. While a very stiff force sensor may not always

exhibit its dynamics, under certain circumstances they may become important. The use of a stiff robot position controller, contact with a stiff environment, or impact with the environment may excite the sensor dynamics. Therefore, it is sometimes necessary to include the sensor in our model. A second-order model of the sensor dynamics can be added to the above models of the arm and environment by placing a spring and damper between the masses of these two second-order systems.

Finally, it is necessary to return to the subject of link stiffness and higher order arm dynamics. It has been recognized by some researchers that the arm has higher order dynamics that may need to be modeled (Roberts 1984; Eppinger and Seering 1986, 1987; Youcef-Toumi and Gutz 1989). This is particularly true if the environment and sensor are stiff. Inclusion of a second-order approximation for the link stiffness makes the composite arm model fourth order, and the arm/sensor/environment model sixth order. However, if the link and sensor dynamic characteristics are similar, they may be lumped together. For instance, a typical force sensor is composed of strain gauges mounted on aluminum. If such a sensor is mounted on an aluminum robot arm, there is no clear distinction between the end of the last link and the beginning of the sensor. Modeling just the first mode of vibration of this entire assembly requires only a second-order model for both the arm links and the force sensor. (This concatenation of the stiffness and damping of both components reduces the total stiffness and damping of the link-sensor by a geometric proportionality factor that depends on the arm and sensor designs [Volpe 1990].) Thus the entire model for the arm-actuator/arm-linkage-and-sensor/environment system can be reduced from sixth to fourth order. This model is shown in Figure 2. The transfer function of this system is:

$$G = \frac{F_m}{F} = \frac{(m_B s^2 + c_3 s + k_3)k_2}{\big(m_B s^2 + (c_2 + c_3)s + (k_2 + k_3)\big)(m_A s^2 + c_1 s + k_1) + (m_B s^2 + c_3 s + k_3)(c_2 s + k_2)} \quad (1)$$

where $F_m = k_2(X_B - X_A)$ is the measure force; x_A is the measured position of the arm; x_B is the position of the environment; and m, k, and c are the mass, stiffness, and damping parameters of the fourth-order model. This is similar to the model presented in Eppinger and Seering (1987).

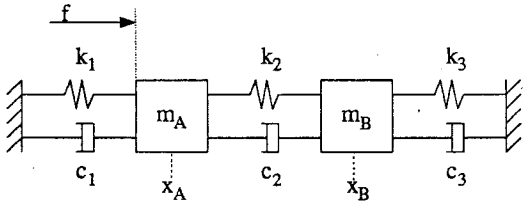

Fig. 2. General fourth-order model of the arm, sensor, and environment system.

We have experimentally extracted parameter values for the components of this model for the described experimental configuration. Theoretical and experimental details can be found in Volpe and Khosla (1990). The pole/zero locations indicated by the extracted values differ greatly from those assumed by other researchers (Eppinger and Seering 1986, 1987). Figure 3 shows all but the leftmost pole, which is at $-28,000$ on the real axis. The complex pole pair is due mainly to the environment. The real pole pair (the real pole shown plus the other not shown) is due mainly to the sensor dynamics. These pole pairs will be called the environment and sensor poles, respectively. It can be seen that the sensor poles are fairly far removed from the environmental ones and are located farther into the left half plane. The leftmost sensor pole will be ignored, as it is negative real and far removed from the others.

4. Explicit Force Control and Impedance Control

The system modeled in the previous section is the plant of the controller used for environmental interaction. Two main conceptual choices have emerged for the choice of this controller structure: *explicit force control* and *impedance control*. It has been shown both theoretically and experimentally that second-order impedance control against a stiff environment is essentially equivalent to proportional gain explicit force control with feedforward (Volpe 1990; Volpe and Khosla 1991b). The argument supporting this conclusion will only be reviewed here.

First, it is necessary to present the block diagrams of

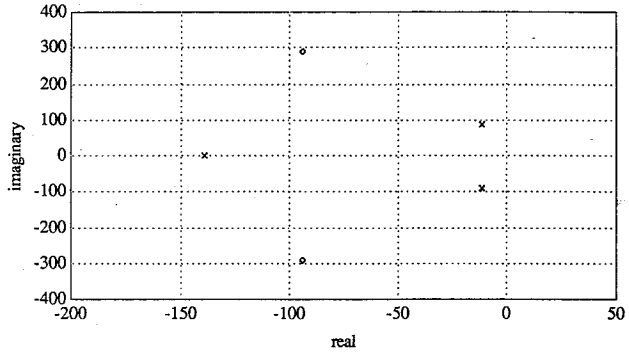

Fig. 3. The pole and zero locations for the fourth-order model using the experimentally extracted parameters. Not shown is the leftmost pole, which is at −28,000 on the real axis.

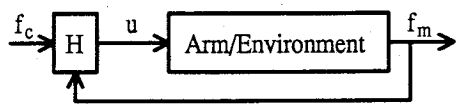

Fig. 4. Explicit force control block diagram.

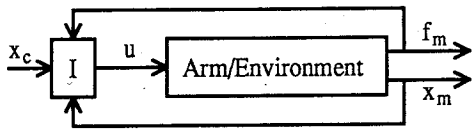

Fig. 5. Impedance control block diagram.

the explicit force and impedance controllers, as in Figures 4 and 5. Next, it is important to recognize that the linear impedance controller may be separated into a position component and a force component, as in Figure 6. Further, Figure 7 shows that because there is no external reference force signal, the force loop may be considered an internal explicit force controller. The type of this internal explicit force controller can be extracted by looking at the impedance control law (Hogan 1985; Volpe 1990):

$$\tau = J^T \Lambda M^{-1}\left[C(\dot{x}_c - \dot{x}_m) + K(x_c - x_m) - f_m\right] - J^T \Lambda \dot{J}\dot{\theta} + h + g + J^T f_m \quad (2)$$

where Λ is the manipulator inertia matrix in Cartesian space; M, C, and K are the second-order impedance matrices; h is the vector of Coriolis and centripetal forces; g is the gravitation force vector; J is the manipulator Jacobian; f, τ, x, and $\dot{x}$ are vectors of force, torque, position, and velocity; and subscripts c and m indicate commanded and measured quantities. The terms that compensate for velocity dependent forces and gravity can be considered feedforward terms and ignored for the remainder of this discussion. What is left is an equation for torque of the form:

$$\tau = J^T\left[H'(f_c - f_m) + f_m - K_v \dot{x}_m\right] \quad (3)$$

$$f_c = K(x_c - x_m) + C\dot{x}_c \quad (4)$$

$$H' = \Lambda M^{-1} \quad (5)$$

$$K_v = H'C \quad (6)$$

The active damping provided by K_v may be added to the passive damping in the plant (c_1 in equation (1)) and removed from further consideration in the control equations.

Thus, the internal explicit force controller in impedance control can be represented by the block diagram in Figure 8, where G is the plant given by equation (1). In this figure, the positive feedback loop acts as a reaction force compensation. If the sensor dynamics are ignored, the physical reaction force loop may be directly extracted from the plant (Volpe 1990). As seen in Figure 9, this creates a new plant, G', and a negative feedback loop of

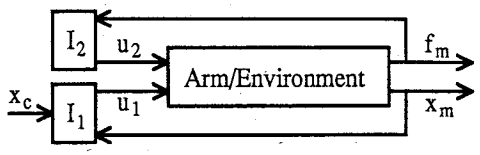

Fig. 6. Impedance control block diagram with the controller divided into its position part, I_1, and its force part, I_2.

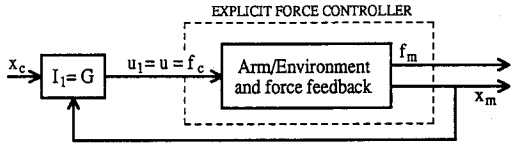

Fig. 7. Impedance control block diagram redrawn to show the inner explicit force controller.

the physical reaction force. Further, this figure shows an equivalent expression of the proportional gain as $H' = H + 1$. The transfer function for this controller is:

$$\frac{F_m}{F_c} = \frac{H'G'}{1 + H'G'} \quad (7)$$

$$= \frac{(H+1)G'}{1 + (H+1)G'} \quad (8)$$

It can be seen directly that an equivalent block diagram of this system may be constructed as in Figure 10. This is a proportional gain explicit force controller with feedforward and serves as the inner force loop in the impedance controller.

When in contact with a stiff environment, the position of the environment can be set as the origin ($x_m = 0$). Also, the commanded velocity is usually zero ($\dot{x}_c = 0$). Thus, the external position loop of the

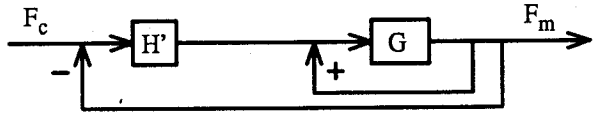

Fig. 8. Block diagram of a force-based explicit force controller with proportional gain and positive feedback for reaction force compensation.

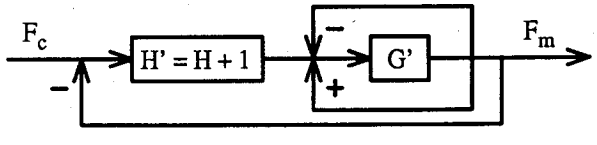

Fig. 9. Block diagram of a force-based explicit force controller with proportional gain and extra feedback for reaction force compensation. The plant G has be expanded into its components, and the sensor dynamics have been ignored.

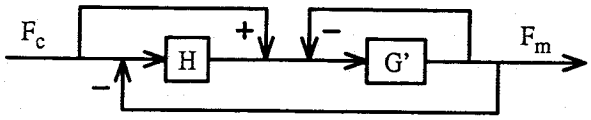

Fig. 10. Block diagram of a force-based explicit force controller with proportional gain and unity feedforward. The plant G has been expanded into its components, and the sensor dynamics have been ignored.

impedance controller provides a command force that is simply $f_c = Kx_c$. The external position loop is, therefore, functionless. We conclude that *for the case of a stiff environment, impedance control is equivalent to proportional gain explicit force control with feedforward.* Elsewhere, we have presented experimental results that support and validate this conclusion (Volpe and Khosla 1991b).

It is interesting to look at what this equivalence implies for gain value selection. (In this discussion, only the one-dimensional or diagonal matrix case will be considered.) First, the stability of the impedance controller is guaranteed for $H' \geq 0$. This is equivalent to the condition $\Lambda M^{-1} \geq 0$. Assuming a constant manipulator inertia Λ, gain H' varies as the inverse of the target impedance mass, M. Zero gain means infinite mass, and large gain means small mass. For the proportional force controller, stable gain values are $H \geq -1$, since $H = H' - 1 = \Lambda M^{-1} - 1$. *Negative proportional force control gains down to -1 are stable.* Further, it will be seen in the next section, that they are desirable for impact control.

5. Impact Control

Impact control is best introduced in a discussion that involves a simplified system without sensor dynamics. After this discussion the sensor dynamics will be included.

5.1. Impact Control Without Sensor Dynamics

The model of the arm/environment plant that neglects sensor dynamics results in pole and zero locations similar to those shown in Figure 3, except the sensor poles are not present. For a proportional gain explicit force controller with this plant, the root locus is shown in Figure 11 ($H \geq -1$). (The poles shown in the middle of the locus are for $H = 0$ and correspond to the environmental pole locations in Figure 3.) Note that one pole will go into the right half-plane for $H < -1$ as predicted. Observing this root locus, it is immediately apparent that the most stable gain is the one that places the two poles at the point where the roots leave the real axis. Ignoring the sensor dynamics, an approximate value of this gain

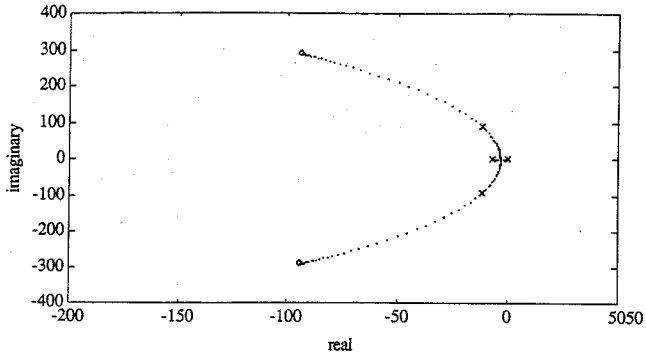

Fig. 11. Root locus for the second-order model for $H' = H + 1$. The double root occurs for $H' \approx 1.5 \times 10^{-3}$. The poles shown in the middle of the locus are for $H = 0$ and correspond to the environmental pole locations in Figure 3.

may easily be determined (Volpe 1990). The double root of the characteristic equation occurs for a value of the proportional gain close to negative one. There are three equivalent ways to view or interpret this result:

1. *Proportional force control with reaction force compensation.* This is the controller in Figure 9. In this case, the controller does not utilize the force error signal, since $H' \approx 0$. However, the reaction force of the impact is directly negated by a feedback signal. Viewed this way, the impact controller does not bounce, because the oscillations in the commanded force and those in the experienced force are equal and opposite. Thus the surface is at a node of two interfering pressure waves. No net force means no net acceleration. Any initial oscillation is damped out by natural and active damping.
2. *Proportional force control with negative gain and a feedforward signal.* This is the controller in Figure 10. While this controller looks different from that above, it has been shown previously that it is equivalent. In this case the controller multiplies the force error by $H = H' - 1 \approx -1$. There is also a feedforward signal of the commanded force.
3. *Impedance controller with a large target mass.* As discussed previously, an impedance controller is equivalent to an explicit force controller when in contact with a stiff environment. Impedance controllers employ a proportional gain, ΛM^{-1}, where Λ is the arm inertia, and M is the desired inertia. Viewed in this way, the impact controller matches the apparent mass of the arm to the stiffness and damping of the environment such that the resultant system is critically damped. More imprecisely, it can be said that the arm is made to appear so massive that it can't bounce.

5.2. *Impact Control With Sensor Dynamics*

Inclusion of the sensor dynamics may change the above analysis somewhat by introducing an additional set of poles. Obviously, if the sensor poles are far from the environmental poles; they will have little effect, and the above results will remain the same. However, the fourth-order model that was previously developed has one pole relatively close to the environmental poles and zeros. Figure 12 shows the root locus for this system for proportional gain values of $-1 \leq H < \infty$ or $0 \leq H' < \infty$. The points of closest approach of the locus to the real axis correspond to gain values of $H \approx -0.8$ or $H' \approx 0.2$. These are the best values for impact control.

It is important to point out that this locus also indicates that positive gain proportional force control, as well as impedance control, will become unstable for this system. The instability of these schemes has been confirmed experimentally (Volpe 1990; Volpe and Khosla 1991b; Volpe and Khosla 1992; Volpe and Khosla 1993a). The points on the locus in the right half-plane correspond to values of $H > 1$ or $H' > 2$. The increase in the oscillatory response of the system presented in the experimentation section of this article indicates this instability. Although the root locus suggests that very high gains would again be stable, experimentation has indicated that the system model breaks down for these large parameter values.

6. Experimental Results

This section presents the results of implementation of the proposed impact control scheme. Both proportional gain explicit force control and impedance control were tested, and the results show their equivalent response. First, however, integral control was implemented, and its poor response is shown.

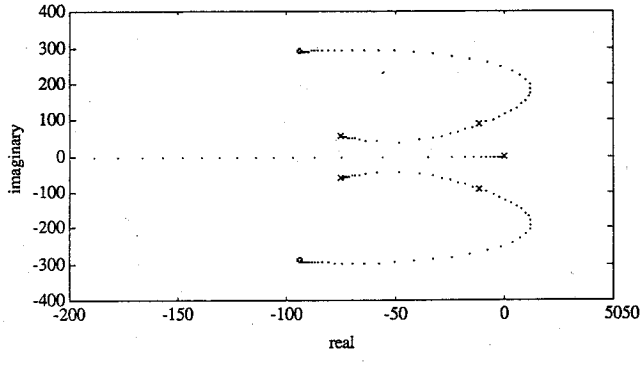

Fig. 12. Root locus for the fourth-order model for $-1 \leq H < \infty$ *or* $0 \leq H' < \infty$. *The poles shown in the middle of the locus are for* $H = 0$ *and correspond to the environmental pole locations in Figure 3.*

The first set of experiments was conducted with the modeled environment of an aluminum plate on a cardboard box. The end effector of the CMU DD Arm II was accelerated toward the environment and struck the hard aluminum surface at the velocity of $\sim$ 75 cm/s. The configuration of the system at the moment of impact is shown in Figure 1. Although dependent on the controller used, the impact force spike was $\sim$ 90 N. For the explicit force control schemes, the force spike from the impact triggered the use of the impact controller. A reference force of 20 N was then supplied.

A velocity gain of $K_v = 10$ was used throughout these experiments. During free-space motion, this value of velocity gain was sufficient for critically damped motion. During contact operations, this value was utilized to maintain consistency with the system model developed previously (Volpe and Khosla 1990) and described in Section 3. However, during contact the added stiffness of the environment causes this active damping value to be insufficient for critically damped motion in the force controlled degrees of freedom. Increasing the damping is not possible with our system because of velocity signal lag, inaccuracies, and noise as discussed in Section 2.1 and elsewhere (Volpe 1990; Volpe and Khosla 1993b).

The control sampling rate for these experiments was 300 Hz. The Lord force sensor is designed to provide raw strain gauge information at 400 Hz. Therefore, sampling of the force data was asynchronous, as every fourth set of data was missed. However, because the sampling rate was an order of magnitude larger than the oscillations of the system, the results are still valid.

In the graphs shown, the measured force is a solid line, the measured velocity is a short dashed line, and the reference force is a long dashed line. In the legends of the graphs, the measured value of the experienced force is called "MezForc_wd"; the reference value of the applied force is call "RefForc"; the measured valued of the Cartesian velocity is called "MezXVel_wd"; the reference value of the end effector position is call "RefP"; and the hybrid control selection parameter is called "SHybrid" (Raibert and Craig 1981). All of these variables are vectors, and the indices follow the conventions of the C computer language.

In the explicit force control experiments, the reference force is multiplied by the hybrid control selection parameter, which is equal to one only after contact with the environment. Also, because the reference force corresponded to the desired force to be applied, and not the desired force to be experienced, multiplication by -1 is necessary. Therefore, in the explicit force control graphs, the long dashed line represents the hybrid control selection parameter, multiplied by the reference force to apply, multiplied by -1.

In the impedance control experiments, the reference force is determined by the difference between the initial position of the environment and the reference position of the arm, multiplied by the commanded stiffness of the arm. This quantity is displayed in the graphs as a long dashed line. The initial position of the environment in the z direction was a constant value of 0.106 m. *After impact*, the reference position of the arm was set to yield a force of 20 N, given the arm stiffness. However, *before impact* the reference position profile was kept the same for all tests, ensuring a consistent impact velocity.

6.1. Integral Control

It has been shown that integral gain explicit force control provides excellent force tracking capability (Volpe 1990). Also, it has been reported by other researchers that integral control is useful for control of impacts (Youcef-Toumi and Gutz 1989). This reference acknowledges that integral control causes the arm to more quickly bounce from and return to the surface. However, it is reported to be a benefit that will shorten the transient period. Our results in Figure 13 indicate otherwise. An increased integral gain increases the rate and magnitude of the bouncing and can lead to instability. After an initial impact with the environment, the manipulator jumps away and strikes on the environment with a larger force the second time. For the gain value used ($K_{fi} = 7.5$), the system eventually settles to the commanded force. For larger gains, it was not possible to attain stability.

This instability is a direct result of integrator wind-up. Immediately after impact, the measured force overshoot

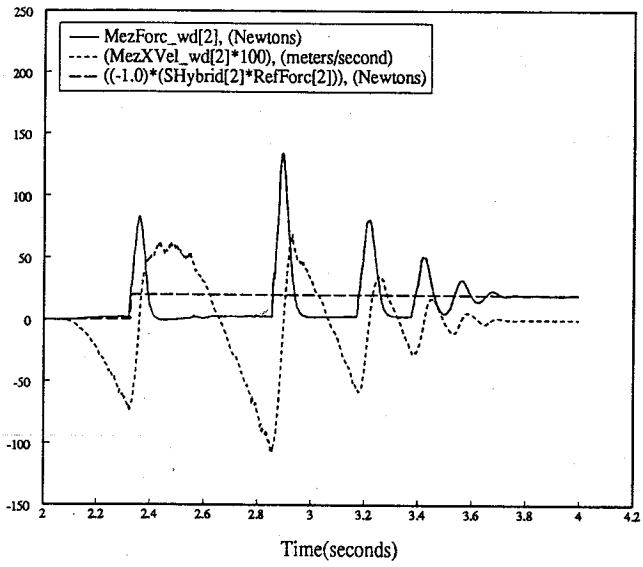

Fig. 13. Experimental data from an impact with integral force control. The integral gain was $K_{fi} = 7.5$.

is large. Therefore, the first error signals to the controller tend to drive the manipulator with a force directed away from the surface (to reduce the error). This actuated force, coupled with the reaction force from the surface, drives the manipulator off the surface. Once off the surface, the measured force drops to zero, and the controller drives the arm into the surface again. For large integral gains, the integrator winds up rapidly, and the forces toward/away from the surface are larger and lead to increased bouncing and instability. For small integral gains, the wind-up is slow and bouncing is smaller, enabling natural and active damping to stabilize the transient. However, even for the extreme of zero integral gain (and, therefore, zero actuation force), the manipulator will likely bounce from the surface because of the natural reaction force from impact.

6.2. Proportional Gain Control with Feedforward

It was predicted earlier in this article that negative proportional gain explicit force control would be stable during impacts. Figure 14 *A–H* shows impact experiments for gain values of $-1 \leq H \leq 0.75$. We have shown previously how negative gains suppress much of the oscillatory behavior of the response when just tracking a force trajectory (Volpe 1990). This is even more true for the impact response. Figure 14 A,B show this suppression of force oscillations even though velocity oscillations continue. In Figure 14 *C–H*, contact is lost with environment as increasing oscillations and repeated impacts occur.

While the stability of the system is best for negative gains, there are two minor drawbacks to their use. First, the magnitude of the impact is increased slightly as $H \rightarrow -1$, as can be seen by comparing parts of Figure 14. This is only important if the environment can not withstand any impacts greater than a particular magnitude. In this case, however, the impact velocity should be reduced. Second, poor steady-state accuracy (after the impact transient) results from the use of negative gains. This is intrinsic to the proportional gain force controller (Volpe 1990). It implies that another controller must be used after the impact phase is over. In previous analysis and experiments we have demonstrated that integral control is best (Volpe 1990).

6.3. Impedance Control

Impedance control was also tested during impacts. Figure 15 *A–C* show the results for the mass ratio $\Lambda M^{-1} = 0.25, 1, 1.75$. The results compare favorably to the responses for proportional force control with $H = -0.75, 0, 0.75$ as shown in Figure 14. This is in direct agreement with theory, as previously discussed, and

once again demonstrates the equivalence of impedance control and proportional gain explicit force control.

Note that to obtain a consistent velocity during the free motion phase, the position gain, K in equation (2), was varied to keep the product $\Lambda M^{-1}K$ constant. The free-space position trajectory was not changed, and the resultant velocity of impact was the same. Also, during and after the impact, the reference position was set such that $K\Delta x = 20$ N. There is, therefore, a discontinuity in the reference position trajectory. The time for the discontinuity was estimated from previous impact trials.

6.4. Discussion of Impact Control Results

The previous sections have shown that an equivalent, stable impact response can be achieved from proper parameter selection for proportional gain explicit force control and impedance control. The appropriate gain values for this particular system are $H \approx -0.75$ for the proportional gain or $\Lambda M^{-1} \approx 0.25$ for the impedance control mass ratio. As discussed previously, these gains are essentially equivalent.

However, gains that are appropriate for impact suppression are not good for force trajectory tracking. It has been shown that the best force trajectory tracking with these controllers is for drastically different gains ($H \approx 0.5$ or $\Lambda M^{-1} \approx 1.5$) (Volpe and Khosla 1991b). Even with these values, the tracking is not close to the performance of integral gain explicit force control (Volpe and Khosla 1992; Volpe and Khosla 1993a).

Further, the impedance control mass ratio that is best for impact control requires very high values of stiffness for free space operation. This can be seen directly from equation (2), in which the mass ratio acts only as a scaling factor to the stiffness and damping when $f_m = 0$. Thus for $\Lambda M^{-1} \approx 0.25$, the stiffness K must be increased by a factor of 4 to obtain the same free-space response. However, this increase in the stiffness may present a problem when the manipulator is in contact with the environment. High stiffness can cause a reduction in the force exerted, as the environment may be compressed and the position error reduced. This situation creates even worse force tracking performance for the impedance controller.

Thus, it is concluded that the best solution is to use three distinct controllers. Position control with properly tuned gains should be used for free-space motion. Impact control, or proportional gain explicit force control with negative gain, should be used to suppress oscillations and bouncing during the transient phase of impact on the environment, and integral gain explicit force control should be used to track forces once stable contact with the environment has been established.

The transition from position control to impact control is abrupt and is triggered by the impact force spike. The transition method from impact control to integral force control is less obvious. One method of doing this is to have a transition period in which the proportional gain and force feedforward of the impact controller are brought to zero, while the integral gain is increased to its best value. We propose a linear switch of all gain values after the impact force pulse diminishes. Determination of the times to begin and end the transition is currently obtained empirically. The beginning and ending gain values are determined from tests of the impact and integral gain force controllers interacting with the same environment (Volpe and Khosla 1992; Volpe and Khosla 1993a).

Figure 16 shows the results of this strategy. The impact control phase lasts for 0.15 s (about the width of the impact spike) after the beginning of the impact. This is followed by a period of transition from impact control to integral gain force control that lasts 0.15 s. During the transition phase, H is varied linearly from -0.75 to 0; K_{ff}, the feedforward gain, is varied linearly from 1 to 0; and K_{fi} is varied linearly from 0 to 15. After this transition period, integral force control is continued with the gain at 15. As can be seen, this simple strategy provides stability through the impact period and excellent position and force control before and after the impact.

6.5. Results With a Stiff Steel Environment

All of the results presented thus far were obtained with the environment model described in Section 3 and developed elsewhere (Volpe and Khosla 1990). To further test the controllers discussed, a very rigid steel pedestal was used as the environment. This pedestal was made from 1-inch-thick steel: two 1-foot-square plates at both ends of a cylinder 34 inches long and 8 inches in diameter. The bottom plate was bolted to a concrete floor. Another piece of steel was bolted to the top plate. It consisted of two $6 \times 1/4$–inch steel plates joined at right angles. (This is commonly called "angle iron.") The angle iron was 1 foot long and provided a vertical surface that was pressed and impacted on.

Two points on this pedestal were used for impact experiments. The first was on the top surface (z direction), directly above the wall of the supporting column. It was the most rigid point on the structure. The pedestal was mounted such that this spot was very close to the Cartesian position at which all previous experiments were performed. The second spot on the pedestal used for experiments was on the face of the angle iron (x direction). This was much less stiff but still considerably more stiff than the previously modeled environment. Its reduction in stiffness from the top surface was due to flexion of the column and weaknesses in the bolted connections.

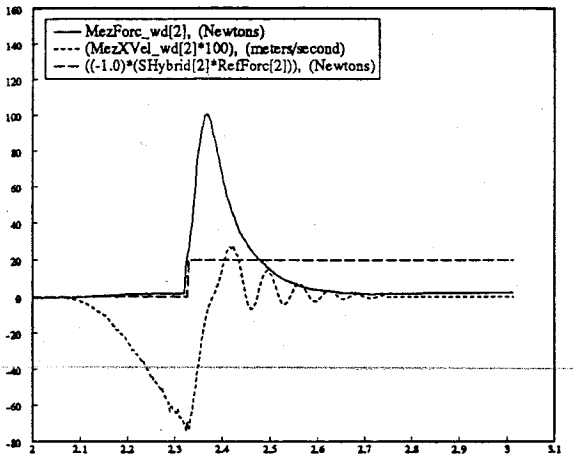

(a) $H = -1$

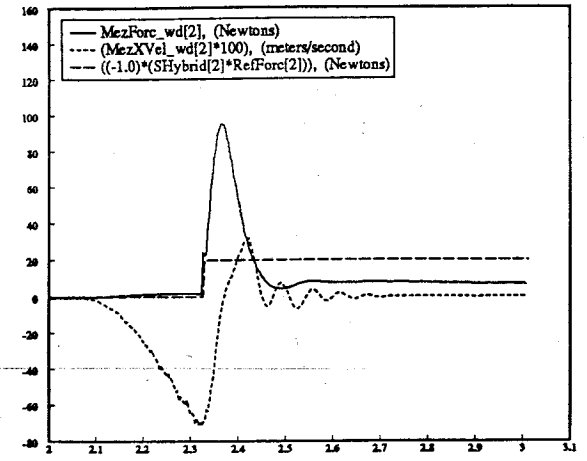

(b) $H = -0.75$

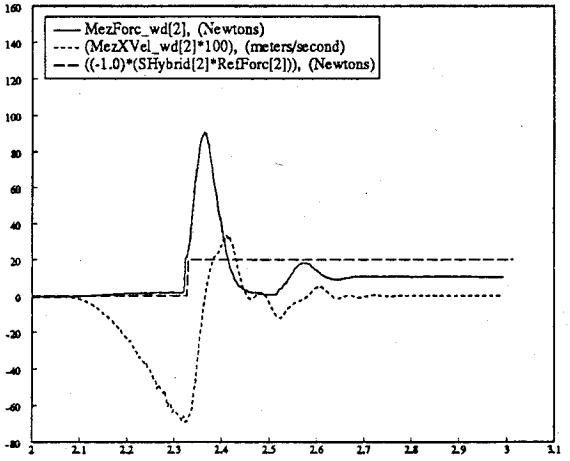

(c) $H = -0.5$

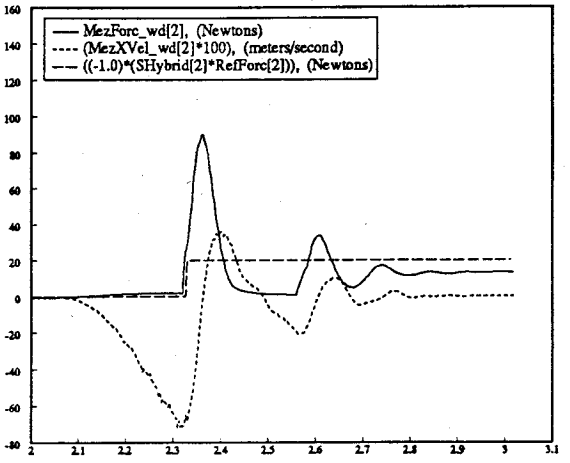

(d) $H = -0.25$

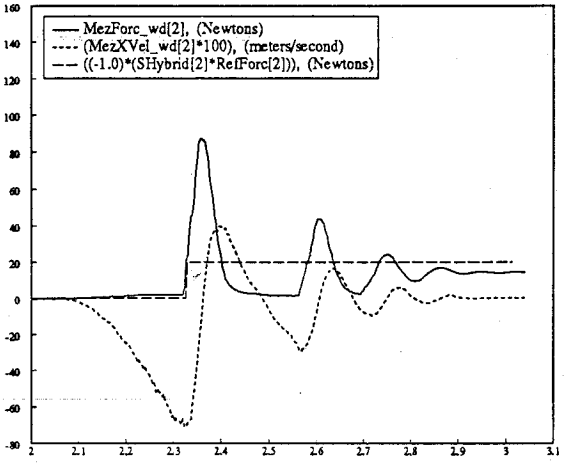

(e) $H = 0$

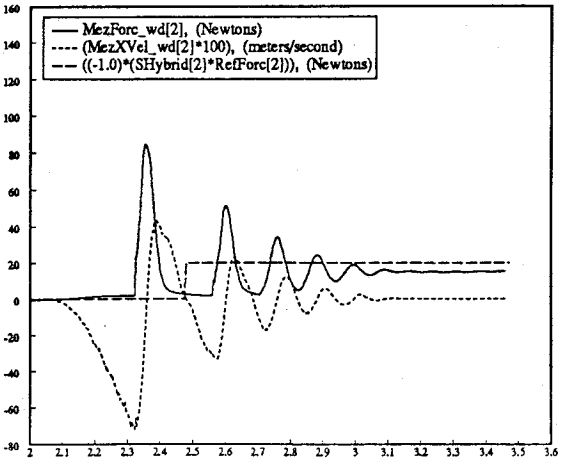

(f) $H = 0.25$

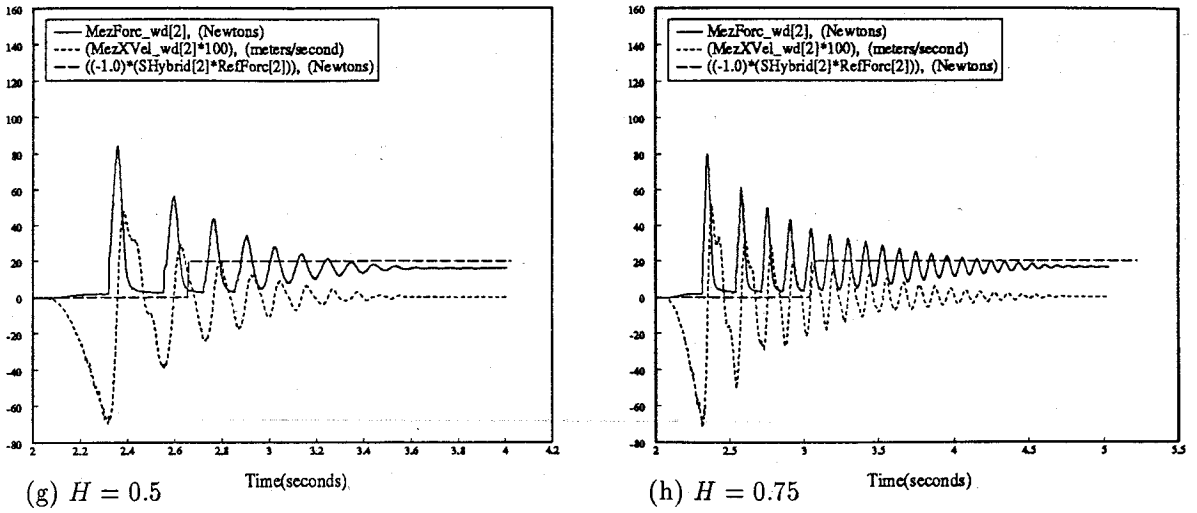

(g) $H = 0.5$ (h) $H = 0.75$

Fig. 14. A–F, Experimental data of proportional gain explicit force control with feedforward during impact. The proportional gain varies from -1 *to* 0.75. *G–H, Experimental data of proportional gain explicit force control with feedforward during impact. The proportional gain varies from* -1 *to* 0.75.

For all impact tests with the steel pedestal, the impact velocity was $\sim$40 cm/s. It proved impossible to prevent bouncing during these tests—at least one bounce would always occur.

Figure 17 shows the response of a z direction impact on the pedestal. The gains compared are for (a) the open-loop case of $H = 0$ and (b) the best impact response at $H = -0.85$. In the case (a), the manipulator bounces several times before coming to rest on the surface. In the case (b), the manipulator bounces but returns slowly and softly to the surface, reestablishing contact in less than 1 s. While the settling time is longer, we prefer the response in (b), as it removes the bouncing behavior of the arm. Repeated impacts resulting from bouncing can lead to damage and degradation of the arm, environment, and sensor.

Figure 18 shows the response of an x direction impact on the angle iron face. The cases compared are for a poor impact response with a positive gain of $H = 0.75$ and the best impact response at $H = -0.75$. Even though both results are oscillatory, it is obvious that the negative gain impact produces peaks that are less numerous and smaller in magnitude. Also, the oscillations diminish more quickly in the negative gain case. Although it is true that the steady-state error of the negative gain case is larger, it has been shown that switching to integral gain control can accomplish accurate tracking very rapidly. For instance, a 0.2-s switching rise time would make the response in (b) begin accurate tracking before the response in (a) had settled from the transient.

In an attempt to improve the response for impacts with the stiff environment, two changes in the system were tried. First, the impacts were tried with and without the brass weight on the end effector. Without the brass weight, it is guaranteed that contact will occur at only one point. Otherwise it is possible that one edge of the brass weight will strike the steel surface first, causing a torque that will cause an impact of the opposite edge to immediately follow. This type of multiple contact can obscure the resultant data. However, removing the weight produced only minor changes in the response.

The second change was to eliminate damping from the force control law by having $K_v = 0$ after impact. This measure eliminates any side effects of the velocity signal lag (Volpe 1990). No difference in the response was observed. The presented results have no damping after impact.

It is apparent from these results that impact with a very stiff environment does not implicitly cause instability for these control schemes. The very stiff environment does, however, make the transition from free-space motion to contact more difficult. It has been shown that the proposed impact control method improves the transient response. However, impact with this very stiff environment does tend to excite higher frequency components of the system that are not modeled and most likely cannot be controlled. For the impact velocity tested, it appears that a better response cannot be obtained with this arm/sensor/environment system. One possible recourse is a redesign of the arm and/or sensor so that higher order dynamics are less likely to be excited. Another possibility is to minimally use a passive energy-absorbing component between the sensor and the environment. Although this would effectively reduce the environmental stiffness to that used in the earlier model (making impact without bouncing possible again), it would also introduce all of

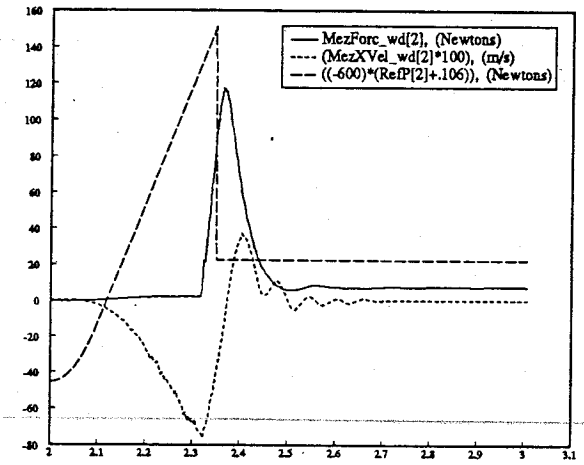

(a) $\Lambda M^{-1} = 0.25$ Time(seconds)

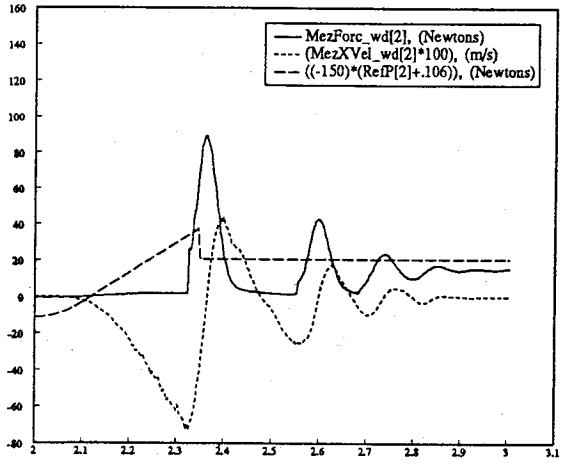

(b) $\Lambda M^{-1} = 1$ Time(seconds)

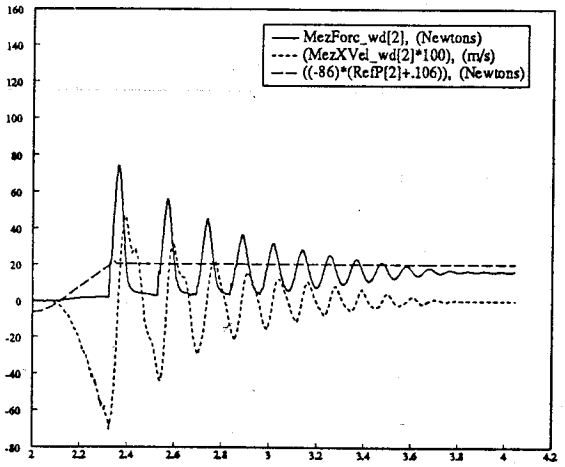

(c) $\Lambda M^{-1} = 1.75$ Time(seconds)

Fig. 15. Experimental data of impedance control during impacts for the stated mass ratios.

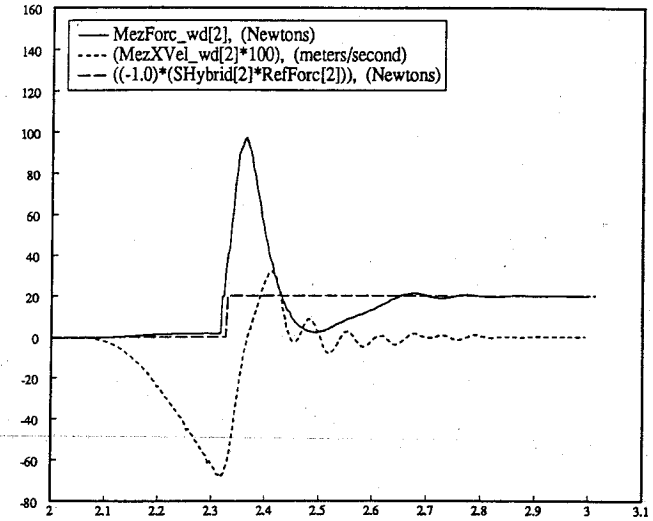

Fig. 16. Experimental data of impact control with transition to integral gain force control. The impact control phase lasts for 0.15s after the beginning of the impact. This is followed by a period of transition from impact control to integral gain force control that lasts 0.15 s. Beyond 0.3 s after impact, integral gain force control is used.

the negative aspects of passive compliance discussed earlier. Probably the best solution would be the introduction of proximity sensing to detect the impending collision and slow the arm to a safer contact velocity. At this slower speed, the higher order dynamics will not be excited during impact.

7. Conclusion

This article has presented a new impact control strategy based on a proportional gain explicit force controller with a feedforward signal and negative gains. It has been shown that this controller is equivalent to impedance control with a large target mass. It is readily apparent that this impact method cannot be used for tracking input force commands, as the input force command is largely ignored. However, it still provides an excellent method of maintaining stability and contact with the environment during the transition from motion through free space to contact with the environment. Once contact has been established and the energy of impact has been dissipated, another force control method (preferably integral gain explicit force control) should be employed.

Acknowledgments

This research was performed at Carnegie Mellon University and supported by an Air Force Graduate Labora-

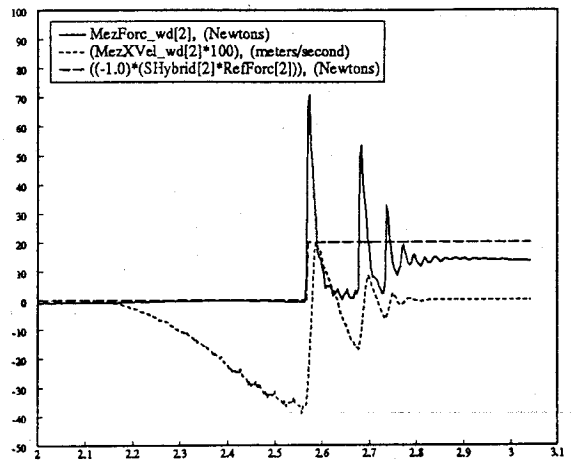

(a) $H = 0$

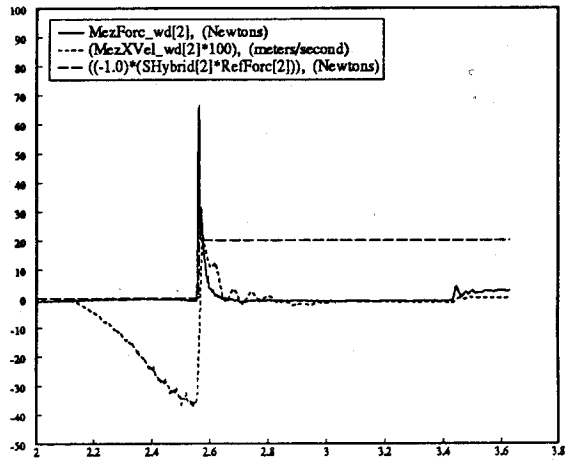

(b) $H = -0.85$

Fig. 17. Impact control on the steel pedestal in the z direction: comparison of $H = 0$ (open loop) and $H = -0.85$.

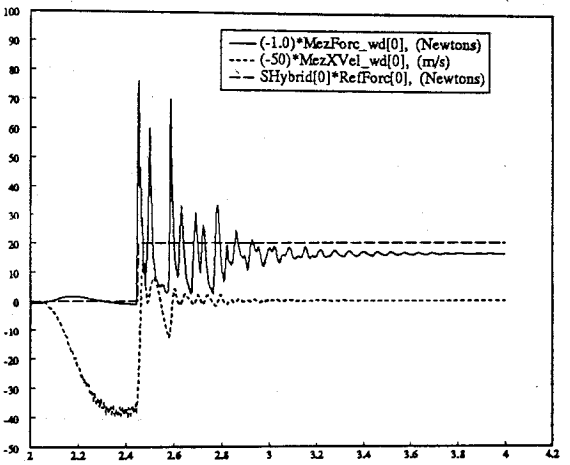

(a) $H = 0.75$

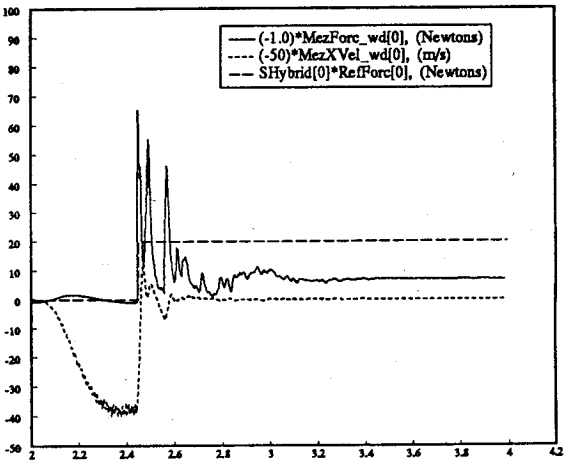

(b) $H = -0.75$

Fig. 18. Impact control on the steel pedestal in the x direction with $H = 0.75$ and -0.75.

tory Fellowship (for R. Volpe), DARPA under contract DAAA-21-89C-0001, the Department of Electrical and Computer Engineering, and The Robotics Institute.

The writing and publication of this article were supported by the above and by the Jet Propulsion Laboratory, California Institute of Technology, under a contract with the National Aeronautics and Space Administration.

The views and conclusion contained in this document are those of the authors and should not be interpreted as representing the official policies, either expressed or implied, of the U.S. Air Force, DARPA, or the U.S. Government. Reference herein to any specific commercial product, process, or service by trade name, trademark, manufacturer, or otherwise, does not constitute or imply its endorsement by the United States Government or the Jet Propulsion Laboratory, California Institute of Technology.

References

An, C., and Hollerbach, J. 1987. Dynamic stability issues in force control of manipulators. *Proceedings of the IEEE Conference on Robotics and Automation*, pp. 890–896.

Colgate, J. E., and Hogan, N. 1988. Robust control of dynamically interacting systems. *Int. J. Control* 48(1):65–88.

De Schutter, J. 1987. A study of active compliant motion control methods for rigid manipulators based on a generic scheme. *Proceedings of the IEEE Conference on Robotics and Automation*, pp. 1060–1065.

De Schutter, J. 1988. Improved force control laws for advanced tracking applications. *Proceedings of the IEEE Conference on Robotics and Automation*, pp. 1497–1502.

Eppinger, S., and Seering, W. 1986. On dynamic models of robot force control. *Proceedings of the IEEE Conference on Robotics and Automation*, pp. 29–34.

Eppinger, S., and Seering, W. 1987 (Raleigh, NC). Understanding bandwidth limitations on robot force control. *Proceedings of the IEEE Conference on Robotics and Automation*, pp. 904–909.

Fu, K., Gonzalez, R., and Lee, C. 1987. *Robotics: Control, Sensing, Vision, and Intelligence*. New York: McGraw-Hill.

Goldenberg, A. 1988. Implementation of force and impedance control in robot manipulators. *Proceedings of the IEEE Conference on Robotics and Automation*, pp. 1626–1632.

Hogan, N. 1985. Impedance control: An approach to manipulation: Parts I, II, and III. *J. Dynamic Sys. Measurement Control* 107:1–24.

Hogan, N. 1987. Stable execution of contact tasks using impedance control. *Proceedings of the IEEE Conference on Robotics and Automation*, pp. 1047–1054.

Hogan, N., and Cotter, S. L. 1982. *Cartesian Impedance Control of a Nonlinear Manipulator*, New York: ASME, pp. 121–128.

Ishikawa, H., Sawada, C., Kawase, K., and Takata, M. 1989. Stable compliance control and its implementation for a 6 D.O.F. manipulator. *Proceedings of the IEEE Conference on Robotics and Automation*, pp. 98–103.

Kahng, J., and Amirouche, F. 1988. Impact force analysis in mechanical hand design—Part I. *Int. J. Robot. Automation* 3(3):158–164.

Kazerooni, H. 1987. Robust, non-linear impedance control for robot manipulators. *Proceedings of the IEEE Conference on Robotics and Automation*, pp. 741–750.

Kazerooni, H., Sheridan, T., and Houpt, P. 1986. Robust compliant motion for manipulators, Parts I and II. *IEEE J. Robot. Automation* RA-2(2):83–105.

Khatib, O. and Burdick, J. 1986. Motion and force control of robot manipulators. *Proceedings of the IEEE Conference on Robotics and Automation*, pp. 1381–1386.

Khosla, P. 1986. *Real-Time Control and Identification of Direct Drive Manipulators*. Ph.D. thesis, Department of Computer and Electrical Engineering, Carnegie Mellon University.

Lawrence, D. 1988. Impedance control stability properties in common implementations. *Proceedings of the IEEE Conference on Robotics and Automation*, pp. 1185–1190.

Maples, J., and Becker, J. 1986. Experiments in force control of robotic manipulators. *Proceedings of the IEEE Conference on Robotics and Automation*, pp. 695–702.

Paul, R. 1987. Problems and research issues associated with the hybrid control of force and displacement. *Proceedings of the IEEE Conference on Robotics and Automation*, pp. 1966–1971.

Paul, R., and Wu, C. 1980 (New Mexico). Manipulator compliance based on joint torque. *IEEE Conference on Decision and Control*, pp. 88–94.

Raibert, M., and Craig, J. 1981. Hybrd position/force control of manipulators. *J. Dynamic Sys. Measurement Control* 103(2):126–133.

Roberts, R. K. 1984. *The Compliance of End Effector Force Sensors for Robot Manipulator Control*. Ph.D. thesis, Department of Mechanical Engineering, Purdue University.

Salisbury, J. K. 1980 (New Mexico). Active stiffness control of a manipulator in Cartesian coordinates. *IEEE Conference on Decision and Control*, pp. 95–100.

Sharon, A., Hogan, N., and Hardt, D. 1989. Controller design in the physical domain (application to robot impedance control). *Proceedings of the IEEE Conference on Robotics and Automation*, pp. 552–559.

Vischer, D., and Khatib, O. 1990. *Design and Development of Torque-Controlled Joints*. Berlin: Springer-Verlag, pp. 271–286.

Volpe, R. 1990. *Real and Artificial Forces in the Control of Manipulators: Theory and Experiments*. Ph.D. thesis, Department of Physics, Carnegie Mellon University.

Volpe, R., and Khosla, P. 1990 (November, Los Angeles). Theoretical analysis and experimental verification of a manipulator/sensor/environment model for force control. *Proceedings of the IEEE International Conference on Systems, Man, and Cybernetics*.

Volpe, R., and Khosla, P. 1991a (April, Sacramento). Experimental verification of a strategy for impact control. *Proceedings of the IEEE International Conference on Robotics and Automation*.

Volpe, R., and Khosla, P. 1991b (June, Toulouse, France). The equivalence of second order impedance control and proportional gain explicit force control: theory and experiments. *Proceedings of the Second Annual International Symposium on Experimental Robotics*.

Volpe, R., and Khosla, P. 1992 (May 10–15, Nice, France). An experimental evaluation and comparison of explicit force control strategies for robotic manipulators. *Proceedings of the IEEE International Conference on Robotics and Automation*.

Volpe R., and Khosla, P. 1993a. A theoretical and experimental investigation of explicit force control strategies for manipulators. *IEEE Transactions on Automatic Control 48(11)*. In press.

Volpe, R., and Khosla, P. 1993b. Computational considerations in the implementation of force control strategies. *J. Intelligent Robot. Sys. Theory Applications*. Special

Issue on Computational Aspects of Robot Kinematics, Dynamics, and Control. In press.

Whitney, D. 1977. Force feedback control of manipulator fine motions. *J. Dynamic Sys. Measurement Control* June:91–97.

Whitney, D. 1985. Historical perspective and state of the art in robot force control. *Proceedings of the IEEE Conference on Robotics and Automation*, pp. 262–268.

Xu, Y., and Paul, R. 1988. On position compensation and force control stability of a robot with a compliant wrist. *Proceedings of the IEEE Conference on Robotics and Automation*, pp. 1173–1178.

Youcef-Toumi, K. 1987. Force control of direct-drive manipulators for surface following. *Proceedings of the IEEE Conference on Robotics and Automation*, pp. 2055–2060.

Youcef-Toumi, K. and Gutz, D. 1989. Impact and force control. *Proceedings of the IEEE Conference on Robotics and Automation*, pp. 410–416.